TELKOMNIKA Telecommunication Computing Electronics and Control
Vol. 24, No. 5, October 2026, pp. 1469~1479
ISSN: 1693-6930, DOI: 10.12928/TELKOMNIKA.v24i5.27664 ❒ 1469

Beamforming design for interference cancellation in fifth-generation new radio system

Heba Shafeik Kashour[1], Abdelrazak Badawieh[1], Ali Ahmad[2], Mohammad Rizk Assaf[3]
[1]Department of Electronics and Communications Engineering, Damascus University, Damascus, Syria
[2]ICTE, Tartous University, Tartous, Syria
[3]Higher Institute for Applied Science and Technology (HIAST), Damascus, Syria

Article Info

Article history:

Received Feb 21, 2026
Revised Jun 4, 2026
Accepted Jun 30, 2026

Keywords:

Channel quality indicator
Eigen-zero forcing
Fifth-generation new radio
Hybrid beamforming
Successive interference cancellation

ABSTRACT

This study proposes a hybrid beamforming (HBF) architecture for interference mitigation design aimed at improving interference cancellation in fifth-generation new radio (5G-NR) systems. The proposed architecture employs interference suppression at two processing level: the linear eigen-zero forcing (EZF) method is applied at the base station (BS) to mitigate inter-user interference (IUI), while the nonlinear successive interference cancellation (SIC) is implemented at each user terminal to cancel intra-user interference. Although EZF is linear, meaning it doesn't require iterative or cumulative operations, its operations are complex and rely on matrix inversion. On the other hand, SIC is a non-linear algorithm, meaning it requires many sequential iterative operations, which increases the probability of cumulative errors. Therefore, using EZF as the first stage makes the signals to be processed in SIC less overlapping, thus reducing cumulative errors, especially under varying channel conditions. The single to interference and noise ratio (SINR) reached a value of 11.9 dB. This is based on the simulation scenarios that were tested. and a channel quality indicator (CQI) value of 10. Moreover, the proposed scheme provides a spectral efficiency of 36 bit/s/Hz at 100 MHz bandwidth and -20 dB signal-to-noise ratio (SNR), achieving performance approaches the performance of a fully digital interference-free system under the considered simulation conditions. while maintaining practical computational complexity.

Corresponding Author:

Heba Shafeik Kashour
Department of Electronics and Communications Engineering, Damascus University
Damascus, Syria
Email: hiba.kashour88@damascusuniversity.edu.sy

1. INTRODUCTION

A new radio access technology (RAT) called fifth-generation new radio (5G-NR) mobile network is developed within the 3rd generation partnership project (3GPP) for 5G [1]. 5G-NR offers globalized standards for the 5G networks with higher capability [2]. Many technologies work together to achieve the expected performance for 5G-NR, these technologies could be summarized as: millimeter waves (mmWave), massive multi input multi output (mMIMO) systems, beamforming (BF) and non-orthogonal multiple access (NOMA) [3].

The use of mm-wave frequency provides access to wider bandwidth than those typically available in conventional cellular system such as long-term evolution (LTE), thereby enabling substantially higher data rates. However, propagation at these frequencies is accompanied by increased pathloss and greater sensitivity to blockage, reflection and absorption by surrounding materials. Consequently, although mmWave transmission can provide high capacity and very hight data rates, its propagation characteristics impose constraints on coverage and link reliability [1].

Multi input multi output (MIMO) techniques can help compensate for some of the propagation limitations associated with mmWave communication. The relatively short wavelength at mmWave reequencies allows a large number of antenna elements to be integrated into a compact physical area, making large-scale antenna arrays practical for mMIMO implementation [4]. In addition to providing spatial diversity, MIMO enables the simultaneous transmission for multiple data streams through spatial multiplexing, thereby increasing the achievable transmission rate [5]. Nevertheless, deploying a fully digital architecture for mmWave mMIMO would require a dedicated radio frequency (RF) chain for each antenna element, resulting in substantial hardware complexity, power consumption, and implementation cost [6]. These limitations motivae the adoption of hybrid beamforming (HBF) architectures.

BF can increase the directivity can result in higher link budget. Consequently, the cell coverage and data rates are improved. Meanwhile, the signal interference can be reduced [5]. In a fully digital MIMO architecture, each antenna element is typically associated with a dedicated RF chain, allowing precoding and combining to be performed entirely in the digital domain. Although this configuration provides substantial flexibility and can approach high spectral efficiency, scalling it to massive MIMO arrays leads to considerable hardware cost and power consumption because of the large number of reqired RF components. Hybrid processing addresses this limitation by combining analog RF processing with a reduced-dimensional digital processing stage [7].

The use of one RF chain for every antenna element becomes impractical in large-scale mmWave mMIMO systems because RF hardware contributes significantly to power consumption, imolementation cost, and physical complexity, particularly at high carrier frequencies [8]. HBF reduces this burden by employing substantially fewer RF chains than antenna elements. Consequently, it provides a compromise between the high array and spatial-multiplexing gains offered by large antenna arrays and the lower hardware complexity associated with a reduced number of RF chains.

The combination of mmWave transmission, mMIMO arrays, and dense small-cell deployment is expected to support high data rates for a large number of users in 5G-NR networks. However, the resulting dense spatial transmission environment can intensify both inter-user interference (IUI) and intra-user interference. Consequently, effective interference management remains an important requirement for maintaining reliable and efficient communication in 5G-NR and beyond.

Interference management techniques can generally be categorized according to their primary objective as interference avoidance, interference explotion, or interference suppression [9]. The proposed work belongs to the third category, where interference is actively reduced either during transmission or through receiver-side processing [10]. In this study, interference suppression is performed through two complementary processing stages: eigen-zero forcing (EZF) is employed at the BS to mitigate IUI, while successive interference cancellation (SIC) is used at the user side to address the remaining intra-user interference.

Early interference-mitigation approaches considered the soatial radiation charateristics of mMIMO antenna arrays, with the objective of concentrating the transitted energy toward the intended direction while limiting undesired sidelobe radiation. Such processing can exploit channel state information (CSI) available at the transmitter. In this context, precoding performs interference suppression before transmission and consequently shifts a substantial part of the signal-processing burden from the receiving terminals to the next generation NodeB (gNB) [11]. Precoding techniques for mMIMO systems can broadly be devided into linear and nonlinear approaches [12]. Linear schemes are generally attractive because of their relatively low computational complexity, although this simplicity may be accompanied by performance limitations under strong interference conditions.

Zero-forcing (ZF) is one of the widely used linear precoding techniques for multi-user interference suppression. It is based on channel inversion and constructs the precoding matrix so that the transmitted signals are spatially directed toward their intended users while placing nills in the directions associated with interfering users. The user data symbols are therefore transformed by the ZF precoding matrixbefore transmissions [12].

The effectiveness of ZF is strongly dependent on the channel condition and noise level, and direct channel inversion may amplify noise when the channel is poorly conditioned. Several modified linear precoding schemes have therefore been investigated to improve this behavior while retaining relatively low complexity. Regularized zero-forcing (RZF) and EZF are examples of such approaches.

Maximum ratio transmission (MRT) is another linear precoding strategy that focuses the transmitted power toward the intended receiver and can prvide near-optimal behavior when IUI is relatively weak compared with noise. In constract, the minimum mean-squre error (MMSE) approach incorporates both interference and noise effects in the precoder design, providing a compromise between the interference suppression capability. of ZF and the signal-gain characteristics of MRT [13]. the underlying objective is to minimize the mean-square erroe between the transmitted symbols and their corresponding received estimates.

SIC is the most common algorithm that suppress the interference by applying filtering mechanism or interference cancellation schemes. It is applying in the combiner part of BF to distinguish different data streams related to single or multi users [14], [15]. Several researchers have attempted to exploit the simplicity and low cost offered by BF designs based on linear interference suppression schemes with proposal procedural improvements that contribute to improving their performance.

Known interference cancellation processes require large and complex calculations to achieve good performance that meets 5G-NR requirements. The novelty lies in integrating EZF for IUI suppression at the BS and SIC for intra-user interference suppression at the user equipment (UE) to balance performance and complexity. Zhao *et al*. [16] the tested the performance of a set of linear precoding algorithms that support interference cancellation using EZF and weighted minimum mean square error (wMMSE). It demonstrated that although linear precoding algorithms have limited performance in multi-user systems, they can perform well when using different architectures. Kaziu *et al*. [17] proposed a decentralized linear-EZF precoding schemes for signal processing at the BS in massive multi-user downlink MIMO systems. Their approach considers simultaneous transmissions of multiple data streams to individual user devices. Nguyen *et al*. [18] investigated an RZF-based BF design aimed at managing multi-user interference while improving the achievable system throughput. Koc and Ngoc [19] introduced a semi-blind MMSE (S-MMSE) technique for reducing residual self-interference by exploiting angle-of-arrival (AOA) information. They further proposed an angular-based joint hybrid precoding and combining (AB-JHPC) scheme for full-duplex mmWave mMIMO systems. Their numerical evaluation showed effective suppression of the self-interference signal, with the reported SIC performance reaching 85.7dB. Abrardo *et al*. [20] presents a distributed digital/hybrid beamformig architecture with MMSE-SIC receivers for MIMO interference channels involving multiple transmitter-receiver pairs. In that framework, a wMMSE-based SIC receiver is employed to mitigate intra-user interference, wherease linear spatial filters are used to suppress interference between different transmitter-receiver pairs. Taricco [21] considers a limited-SIC strategy as an alternative to the full SIC procedure commonly used in NOMA systems. The study evaluates the effect of restricting the number of SIC staes on system performance and derives the corresponding power-allocation coeffients under the adopted optimization criterion. This approach is particularly relevant to terminals with imited computational resources, where performing a complete SIC process can become prohibitively complex as the number of users served by the same BS increases.

From an implementation perspective, the computational requirements of linear interference-cancellation techniques can make their deployment at resource-constrained used devices undesirable. Accordingly, such processing can be assigned to the BS to suppress interference among different users. In contrast, the sequential nature of SIC requires channel information for successive detection and demodulation, making it suitable for processing the multiple streams associated with an individual user. Based on this distinction, the proposed architecture performs EZF-based IUI suppression at the BS and applies SIC at the UE for intra-user interference cancellation. The proposed dual-stage interference cancellation achieves an SINR of 11.9 dB, a channel quality index (CQI) of 10, and a spectral efficiency 33 bit/s/Hz.

2. METHOD

Figure 1 illustrates the considered a mmWave mMIMO hybrid BF system for 5G-NR. At the transmitter N_s inepenent spatial streams conveyed through N_t antennas using N_t^{RF} RF chains. At the receiver, the signal is collected by N_r antennas and processed through N_r^{RF} RF chains. The hybrid architecture is designed to reduce hardware and processing complexity; therefore, the number of RF chains is constrained to remain below the corresponding number of antenna elements. Accordingly, the number of transmitted spatial streams satisfies $N_s \leq N_t^{RF}(N_r^{RF}) \leq N_t(N_r)$. At each side of the link, an RF chain is connected to the corresponding set of phase shifters. This connection enables each RF chain to form a beam for transmitting or receiving an independent spatial data stream. After hybrid precoding, the resulting transmit vector propagates through the mmWave channel H, producing the received signal vector y. The receiver then applies the hybrid combining matrix $W^* = W_{BB}^* W_{RF}^*$, where W_{BB}^* and W_{RF}^* denote the baseband and RF combining matrices, respectively. The resultant signal at the receiver is in (1):

$$\hat{y} = \sqrt{\rho}\ W_{BB}^* W_{RF}^* H F_{RF} F_{BB} S + W_{BB}^* W_{RF}^* \tag{1}$$

In (1) S represents the vector of transmitted symbols and ρ specifies the average received-signal power. The matrices F_{BB} and F_{RF} denote the digital baseband and analog RF precoders, respectively, with dimensions $[N_t^{RF} \times N_s]$ and $N_t \times N_t^{RF}$. For multi-user transmission F_{BB} is organized into user-specific submatrices denoted by F_{BB1}, F_{BB2},…., $F_{BB,K}$, with each component corresponding to one of the served users. associated with the served users.

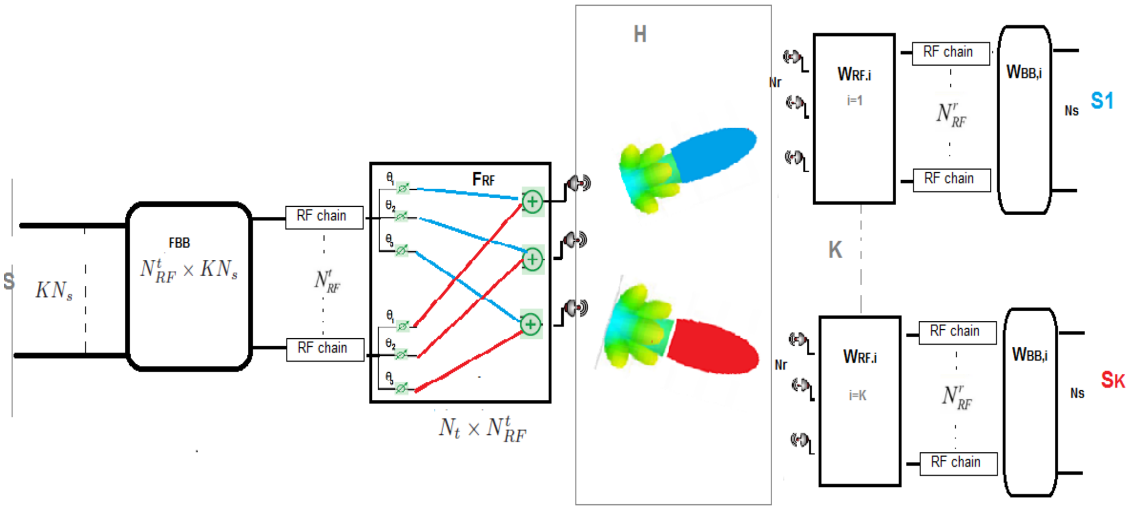

Figure 1. mmWave mMIMO hybrid BF system for 5G-NR

The RF precoder F_{RF} is implemented using phase-shifting elements; consequently, its entries are constrained to have constant magnitude, while their phases can be adjusted to control the transmitted signal direction. The channel model is normalaized according to the adopted system parameters, where H denotes the mmWave propagation channel. The additive noise vector n, of dimestion $(N_r \times 1)$, is modeled as a zero-mean complex Gaussian vector with covariance matrix $\sigma^2 I_{Nr}$. At the receiver, the overall combining matrix is obtained from the cascade of the RF and baseband combiners and is expressed as $W_{BB}^* W_{RF}^*$, where $W_{BB}(N_r^{RF} \times N_s)$ denotes the baseband combiner and $W_{RF}(N_r \times N_r^{RF})$ represents the analog RF combiner. For characterizing the mmWave MIMO channel, we employ the extended Saleh-Valenzuela geometric model [22]. In this representation, the propagation environment is described by N_{cl} scattering clusters, with each cluster containing N_{ray} propagation paths. The contributions of these pathes are combined to construct the channel matrix H. Accordingly, the discrete-time narrowband channel representation can be formulated as given in (2).

$$H = \sqrt{\frac{N_t N_r}{N_{cl} N_{ray}}} \sum_{i=1}^{N_{cl}} \sum_{l=1}^{N_{ray}} \alpha_{i,l} a_r(\emptyset_{i,l}^{\gamma}) a_t(\emptyset_{i,l}^{t}) \quad (2)$$

where $\alpha_{i,l}$ denotes the l^{th} ray complex gain in the i^{th} cluster. $a_r(\emptyset_{i,l}^{\gamma})$ and $a_t(\emptyset_{i,l}^{t})$ denote the l^{th} ray array response vectors at the receiver and transmitter in the i^{th} cluster, with azimuth angles $\emptyset_{i,l}^{\gamma}$ and $\emptyset_{i,l}^{\gamma}$, respectively. As observed, the channel matrix $\mathrm{H} \in \mathbb{C}^{N_r \times N_t}$ normalized to satisfy $\mathrm{E}\{\|\mathrm{H}\|_F^2\} = N_t N_r$. To simplify representing channel matrix, we rewrite it in a more compact form as:

$$H = A_r diag(\alpha) A_t^* \quad (3)$$

where $\alpha = \sqrt{\frac{N_t N_r}{N_{cl} N_{ray}}} [\alpha_{1.1}, \alpha_{1,2}, \dots, \alpha_{N_{cl} N_{ray}}]^T$ contains the complex gains of all paths, and the matrices $A_r = [a_r(\emptyset_{1,1}^{\gamma}), a_r(\emptyset_{1,2}^{\gamma}), \dots, a_r(\emptyset_{N_{cl},N_{ray}}^{\gamma})]$ and $A_t = [a_t(\emptyset_{1,1}^{t}), a_t(\emptyset_{1,2}^{t}), \dots, a_t(\emptyset_{N_{cl},N_{ray}}^{t})]$ contain the array response vectors. As a result, the number of the paths is the upper bound of the rank of the mmWave channel matrix. The primary challenge in hybrid structure is designing precoding and combining matrices in order to maximize the spectral efficiency R:

$$R = log_2 \left(\left| I_{Ns} + \frac{\rho}{N_s} R_n^{-1} W_{BB}^* W_{RF}^* H F_{RF} F_{BB} \times F_{BB}^* F_{RF}^* H^* W_{RF} W_{BB} \right| \right) \quad (4)$$

To achieve a favorable trade-off between the achievable spectral efficiency and the computational complexity of the multi-user hybrid RF BF scheme, aphase-based design is adopted for the RF precoder and combiner [23]. Accordingly, the spectral efficiency associated with the i-th data stream of the k-th MS can be expressed as:

$$R_{k;i} = log_2\left(\left|1 + SINR_{k;i}\right|\right) \quad (5)$$

By aggregating the specral efficiencies of all data streams across the served users, the overall sum spectral efficiency is obtained as follows:

$$R = \sum_{k=1}^{K} \sum_{i=1}^{N_s} log_2\left(\left|1 + SINR_{k;i}\right|\right) \quad (6)$$

where $SINR_{k,i} = \frac{P_S}{P_n + P_I}$ denotes SINR of the i-th stream of the k-th user. Ps, P_I and P_n are the desired signal power, interference power and noise power. The main purpose of this paper is to maximize the sum spectral efficiency of all users under total transmit power and constant modulus constraints on each entry of the analog beamformers, assuming perfect knowledge of H_k .

2.1. Suppress IUI in precoder side

According to (1), the signals corresponding to different spatial streams may remain coupled at the outputs of the matched filters. The ZF detector addresses this coupling by applying the inverse of the channel matrix to the received observation, there by separating the multiplexed data streams. A major limitation of conventional ZF detection is that channel inversion can amplify the noise component at the detector output, particularly for unfavorable channel condition [24]. EZF addresses this limitation by exploiting the eigenvalue characteristics of the channel-related matrix to constrain noise enhancement and improve the resulting detection performance. For independent and identically distributed input noise samples, the average noise power at the ZF detector output does not excedd the corresponding input noise power when the sum of the expected eigenvalues satisfies the condition given in (7). In this expression

$$\bar{P}_{ny} \leq \bar{P}_{nx} \leftrightarrow \sum_{n=1}^{N} E[\lambda_n] \leq N \quad (7)$$

$\bar{P}_{nx}$ and $\bar{P}_{ny}$ denote the average noise power before and after ZF detection, respectively, λ_n represent the nth eigenvalue of the specified inverse-channel matrix $[H^{-1}.(H^{-1})^H]$.

Siddiqui *et al.* [24] investigated the use of adaptive transmit- and receive- antenna gains to control the channel characteristics and satisfy the required eigenvalue condition. Three gain-adjustment configurations were considered. The first assumes that CSI is available at the transmitter through a feedback link, allowing the transmit gains to be optimized according to the channel information. In the second configuration, the transmit gains are fixed while the receiver adjusts its antenna gains. The third jointly optimizes the transmit and receive gains. According to the reported analysis, appropriately adjusting these gains brings the eivenvalues of the inverse channel matrix closer to the required condition, thereby reducing the noice enhancement associated with RF detection and allowing its performance to approach of the maximum likelihood (ML) detector.

$$\sum_{n=1}^{N} E\left[\lambda_{Qn}\right] \leq N \quad (8)$$

λ_{Qn} is the nth eigenvalue of the random matrix $[H^{-1}.(H^{-1})^H]$.

After obtaining the effective channel representation for each UEs, the associated eigenvectors are employed to determine the spatial processing required for multi-user ZF processing. In this approach, the spatial characteristics of the channel covariance are exploited to identify suitable BF directions. For the k-th UE, the channel matrix is represented throught its singular-value decomposition (SVD). In (9), the matrices U_k and V_k contain the corresponding left ad right singular vectors, wherease A_k is the diagonal matrix formed bythe associated singular values [25].

$$H_k = U_k\, A_k V_K^H \quad (9)$$

$$Z_{k,ave} = V_k A_k A_k^T\, V_k^T$$

The singular-value matrix associated with the k-th UE is denoted by A_k and is gived by: $A_k = diag(\sqrt{\lambda_1}, \sqrt{\lambda_{2\,,}} \dots \dots, \sqrt{\lambda_r})$ assuming that $\sqrt{\lambda_1} \geq \sqrt{\lambda_2} \geq \cdots \sqrt{\lambda_{r1}} \in R$ is ith largest eigenvalue of the current UE channel matrix, and Uk and Vk are semi-unitary matrices so that $U_k^H U_k = IR$ and $V_k^H V_k = I_M$. Unitary property also means that the columns of Uk and Vk are orthogonal. The right-hand side semi-unitary matrix of V_k for UE_k can be formed as:

$$V_k = [V_{k1}, V_{k2}, \dots \dots]^T \tag{10}$$

and BF weights for each UE is defined as:

$$W_i = V_i \; i = 1,2, \dots ., K$$

The right singular vectors onbtained from the channel decomposition are subsequently used to constract the BF weights. By combining the relevant vectors for all UEs, an equivalent channel matrix H_{eq} is obtained as defined in (11).

$$H_{eq} = (V_{11}, V_{21}, \dots, V_{K1})^H \tag{11}$$

Channel knowledge is typically assumed at the receiver for the coherent combining. Therefore, diversity gain depends on the H availability at the transmitter. When H matrix is known to the transmitter, received signal-to-noise ratio (SNR) is optimized by using precoding and receiver weights matrices according to V and U matrices respectively.

2.2. Suppress intra-user in combiner side

To perform SIC across the multiple streams associated with the k-th mobile station (MS), the baseband combining matrix is constructed from the effective channel according to the following defenation of $G_k(H_k^{\sim H}.H_k^{\sim H})^{-1}H_k^{\sim H}$. The i-th row of the resulting combiner is then used to detect the corresponding data stream of the k-th MS is $W_{BB,k}^H(i,:) = G_k(i,:)$. The detected i-th data stream of the k-th M $s_{k,i}^{\sim}$ is given by (12):

$$\begin{aligned} s_{k,i}^{\sim} &= W_{BB,k}^H(i,:)y_{RF,k} \\ &= W_{B,k}^H(i,:)W_{RF}^H.H_k\,.F_{RF}.F_{BB,k}(:,i)s_{k,i}^{\sim} + W_{BB,k}^H(i,:)W_{RF}^H\; n_k \end{aligned} \tag{12}$$

As shown in (12), the received expression can be separated into the desired i-th stream and the effective noise component. the choice of $W_{BB,k}^H(i,:) = G_k(i,:)$. removes the contribution of the other streams belonging to the same user. The detected symbolis subsequently demodulated and re-modulated so that its reconstructed conteibution can beremoved from the received signal during the SIC process. The reconstructed symbol is thensubtracted from the received signal to obtain an updated observation in which the detected stream is removed. The resulting signal, given by (13), contains the remaining streams and the receiver noise and is subsequently used for detection of another streams.

$$\begin{aligned} y_{k,i}^{\sim} &= y_{RF,k} - h_{k,i}^{\sim}\, s_{k,i}^{\sim} \\ &= \sum_{j=1, j\neq i}^{Ns} H_k^{\sim}\,.F_{BB,k}(:,j)s_{k,j} + W_{RF,k}^H\; n_k \end{aligned} \tag{13}$$

Next, we will detect the n-th ($n \neq i$) data stream of the k-th, MS sk, n.

The completed processing procedure can be summarized as follows. For each user k, the analog combiner is obtained from the first N_{RF}^r left singular vectors of H_k. The RF precoder is constructed from the first N_{RF}^t right singular vectors of H_{eq}.

The corresponding digital precoder is then obtained from the right singular vectors of the effective channel, while the digital combiner is determined from the G_k matrix used for stream detection. H_k is given according to (9) and H_{eq} is given according to (11). Analog stage: for k: from 1 to K: $\{W_{RF,k} = U_k^{(N_{RF}^r)}$; $U_k^{(N_{RF}^r)}$ is consists of the first N_{RF}^r left singular vectors of $H_k\}$. Digital stage: for k: from 1 to K: $\{F_{RF,k} = V_{int}^{(N_{RF}^t)}$; $V_{int}^{(N_{RF}^t)}$ consists of the first N_{RF}^t right singular vectors of H_{eq}. $F_{BB,k} = \bar{V}_k^{(N_{RF}^r)}.W_{BB,k}(i,:) = \bar{G}_{k,i}(i,:)\}$.

2.3. Detection stream order

The proposed receiver follows the detection streams ordering (DSO) recommended in [21]. Under the considered NOMA ordering principle, a receiver first decodes the signals associated with weaker users before detecting its own signal. Although the receiver may determine the decoding sequence independently, the proportional-fairness criterion favors thisv ordering rule. The BS conseqently relies on the adopted order when determining the power allocation for the duperposed transmitted signal.

3. RESULTS AND DISCUSSION

The experimental implementation of the proposed design for interference cancellation was carried out using a hybrid combination of the linear EZF algorithm and the nonlinear SIC algorithm, according to the parameters specified in Table 1 and channel parameter specified in Table 2.

Table 1. Simulation parameters for the performance testing of the proposed design for interference cancellation using a hybrid combination

Simulation medium	Code	Value
Cell diameter	Dr	1000 m
gNB transmit power	PTx	40 dBm
Frequency carrier	Fc	28 GHz
Band width	BW	[20, 140] MHz
Number of antennas at the transmitting end (BS)	Nt	256
Number of antennas at the receiving end (user side)	Nr	64
Number of radio chains at the receiving end (user side)	N_{RF}^{r}	4
Number of radio chains at the transmitting end	N_{RF}^{t}	40
Channel model	Channel model	CDL-D-3GPP TR:38.901
Modulation rank	Quadrature amplitude modulation (QAM) order	64 QAM

Table 2. Clustered delay line D (CDL-D) channel parameter (TR 38.901-Table 7.7.1-1)

Parameter	Value
Number of clusters	12
Dealay spread (RMS)	300 nsec
Maximum delay	1000 ns
Angular spread zentith (ZoD)	22 deg
Angular spread zentith (ZoA)	5 deg
K-factor	0 (NLOS)
Cross polarization power ratio (XPR)	7 dB
Number of rays per cluster	7

3.1. Signal-to-interference and noise ratio indecator

Figure 2 shows the SINR based on the bandwidth used in the system for both the proposed hybrid interference cancellation design and designs that rely on a single method using the linear EZF-HBF algorithm presented by Hassan and Saleh [9], or the single-mode sequential interference cancellation algorithm (SIC-HBF) as described by Gómez-Cuba and Pena-Sande [11].

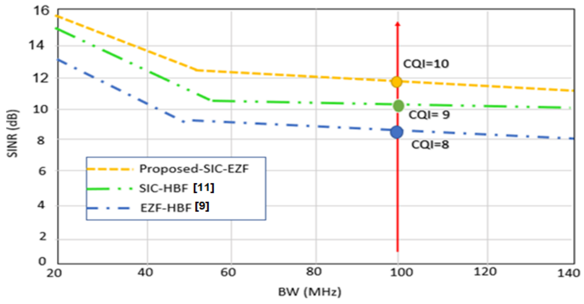

Figure 2. Signal to interference and noise ratio with field width (searcher)

A larger bandwidth allows for the transmission of a larger amount of data, but at the same time, signal quality is reduced due to increased noise and interference. In new 5G radio systems, in accordance with the recommendations of the 3GPP, a CQI has been established. This CQI is determined based on a set of indicators, the most important of which is the SINR at a specific bandwidth and modulation level. Table 3 shows the standard values for the CQI. The higher the CQI value, the greater the likelihood of selecting a higher coding rate and modulation level, and consequently a higher data transfer rate.

Table 3. Standard values for the CQI according to BW=100 MHz bandwidth in 5G-NR systems (3GPP technical specification (TS) 38.214)

Throughput trend	Coding rate	SINR	QAM	CQI
High	0.64	8.6-10.3	64 QAM	8
High	0.77	10.3-11.7	64 QAM	9
Very high	0.88	11.7-13	64 QAM	10
Very high	0.96	13-14.8	64 QAM	11

A good SINR can help achieve higher spectral efficiency because it enables decoding of higher modulation schemes. Network operators always strive to achieve higher spectral efficiency by raising the SINR at all locations to provide the best possible user experience. This can be achieved either by transmitting at higher power (higher transmit power), which is a costly option in practice, or by reducing interference and noise. In some technologies, this interference is leveraged to improve signal quality. According to the measured SINR values shown in Figure 2 and compared with the standard values specified in Table 3, and when the bandwidth is equal to (100 MHz), the proposed algorithm achieves ($SINR = 11.9$), which corresponds to a CQI value ($CQI = 10$). This value allows for reaching a very high data rate at a coding rate close to 0.88. When using SIC-HBF to eliminate interference between data streams, whether belonging to a single user or a group of users, a value of ($SINR = 10.4$) is recorded, which corresponds to a value of CQI ($CQI = 9$), which allows for achieving a high data rate at a symbol rate close to 0.77. When using EZF-HBF, a value of ($SINR = 8.6$) is recorded, which corresponds to the minimum standard value expected when using 64 QAM modulation order with a bandwidth of 100 MHz, and a value of CQI ($CQI = 8$) is recorded, which allows for achieving a high data transfer rate at a symbol rate close to 0.64.

3.2. Spectral efficiency index test with variable SNR values

From a spectral efficiency perspective at various SNR values, the proposed dual-stage architecture outperforms other hybrid designs that operate on a single interference cancellation algorithm, either SIC or EZF. This reflects the proposed design's superior interference cancellation performance, but it should be noted that interference is not completely eliminated. The interference-free system still outperforms the proposed design. According to the simulation results shown in Figure 3, the fully digital BF system maintains a performance advantage in all other scenarios. The difference between the digital and hybrid systems' performance is attributed to the accuracy of the phase shifters used in the analog stage of the hybrid system, which has a 2-bit accuracy. The performance of the tested hybrid systems could be closer to that of the fully digital system if better-accurate phase shifters were used, but this would come at the expense of greater computational complexity and increased hardware cost.

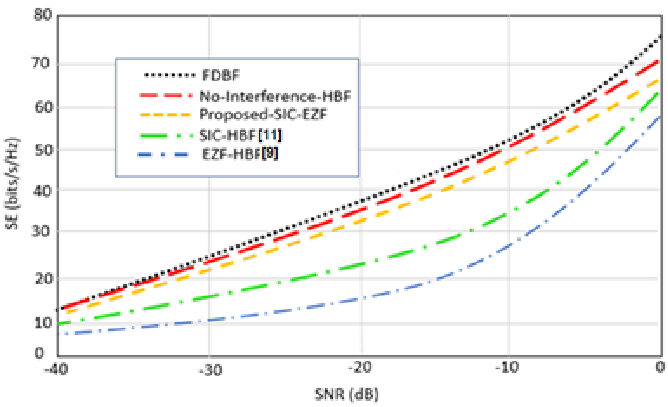

Figure 3. Spectral efficiency with changes in SNR values

3.3. Evaluation of the computational complexity of the integrated model

Table 4 compares the computational complexity of the proposed architecture with the SIC-based scheme in [21] and the EZF-based approach in [17]. The linear algorithms outperform the proposed algorithm and the nonlinear algorithms in terms of simplicity. The complexity of the linear EZF algorithm is related to the number of radio chains at the transmitting end (NRF), which, under the design conditions, is less than the number of transmitting antennas (Nt). However, the complexity of the proposed design and the

SIC-based designs are similar, as both are related to the number of transmitting antenna array elements (Nt). Therefore, it can be said that the proposed algorithm improves performance without adding significant computational complexity to the nonlinear algorithms.

Table 4. Complex degree for proposed HBF

Algorithm	Complex degree
Proposed algorithm	$O(K(N_t N_s^2 + N_s^3) + K^2 N_s N_r^2)$
SIC-HB [21]	$O(K^2 N_t^2 N_r + K N_s N_r^2)$
EZF-HBF [17]	$O(N_t K^2 N_s + K^3 N_s^3)$

3.4. Discussion

The optained results confirm that integrating EZF and SIC in a hybrid BF framework offers an optimal balance between signal quality, spectral efficiency, and system complexity. The EZF stage improves robustness against channel noise and correlation, providing stable precoding performance even under imperfect CSI. The SIC stage ensures accurate stream separation within each user, significantly reducing intra-user interference. Together these stages lead to measurable improvements in SINR, CQI, and even throughput, making the system siutable for real-world 5G-NR application such as massive connectivity, mmWave backhoal, and high-density urban networks.

4. CONCLUSION

The results support the use of a hybrid BF architecture that strategically distributes computational tasks between the BS and UE. specially, it is recommended to implement EZF based processing at the BS to efficiently mitigate IUI, while employing SIC at the user side to address IUI, given its reliance on accurate per-stream CSI. The proposed framework demonstrates notable improvements in spectral efficiency SE of up to 33 bits/s/Hz with $SNR = -20$ dB approaches the performance of a fully digital interference-free system under the considered simulation conditions. In addition, it achieves SINR of up to 11.9 with $BW = 100$ MHz, that matching with $CQI = 10$ which allow to use higher code rate compared with the other scenarios. The proposed work achieves improved performance without introducing excessive additional computational complexity, making this as a practical solution for 5G-NR deployments. It is recommended for scenarios where the number of data steams is limited relative to the number of radio chains in the BS, such as initial access and mobility. In future work, we hope to leverage artificial intelligence (AI) tools to CSI and interference information from users to achieve a more accurate BF matrix. In addition of using integrating reinforcement learning for adaptive BF, applying the design to multi-cell scenarios, or incorporating hardware impairments into simulations.

FUNDING INFORMATION

Authors state no funding involved.

AUTHOR CONTRIBUTIONS STATEMENT

This journal uses the Contributor Roles Taxonomy (CRediT) to recognize individual author contributions, reduce authorship disputes, and facilitate collaboration.

Name of Author	C	M	So	Va	Fo	I	R	D	O	E	Vi	Su	P	Fu
Heba Shafeik Kashour	✓	✓	✓	✓	✓	✓		✓	✓	✓				
Abdelrazak Badawieh	✓							✓		✓	✓	✓	✓	
Ali Ahmad	✓									✓	✓	✓		
Mohammad Rizk Assaf		✓			✓		✓		✓		✓			

C : **C**onceptualization
M : **M**ethodology
So : **So**ftware
Va : **Va**lidation
Fo : **Fo**rmal analysis
I : **I**nvestigation
R : **R**esources
D : **D**ata Curation
O : Writing - **O**riginal Draft
E : Writing - Review & **E**diting
Vi : **Vi**sualization
Su : **Su**pervision
P : **P**roject administration
Fu : **Fu**nding acquisition

CONFLICT OF INTEREST STATEMENT

Authors state no conflict of interest.

DATA AVAILABILITY

The datasets generated and/or analyzed during the current study are available from the corresponding author upon reasonable request.

REFERENCES

[1] A. A. Zaidi *et al.*, "Waveform and Numerology to Support 5G Services and Requirements," *IEEE Communications Magazine*, vol. 54, no. 11, pp. 90–98, Nov. 2016, doi: 10.1109/MCOM.2016.1600336CM.

[2] F. Rinaldi, A. Raschellà, and S. Pizzi, "5G NR system design: a concise survey of key features and capabilities," *Wireless Networks*, vol. 27, no. 8, pp. 5173–5188, 2021, doi: 10.1007/s11276-021-02811-y.

[3] F. Boccardi, R. W. Heath, A. Lozano, T. L. Marzetta, and P. Popovski, "Five disruptive technology directions for 5G," *IEEE Communications Magazine*, vol. 52, no. 2, pp. 74–80, Feb. 2014, doi: 10.1109/mcom.2014.6736746.

[4] R. Dilli, "Hybrid Beamforming in 5G NR Networks Using Multi User Massive MIMO at FR2 Frequency Bands," *Wireless Personal Communications*, vol. 127, no. 4, pp. 3677–3709, 2022, doi: 10.1007/s11277-022-09952-z.

[5] S. Lavdas, P. K. Gkonis, Z. Zinonos, P. Trakadas, L. Sarakis, and K. Papadopoulos, "A Machine Learning Adaptive Beamforming Framework for 5G Millimeter Wave Massive MIMO Multicellular Networks," *IEEE Access*, vol. 10, pp. 91597–91609, 2022, doi: 10.1109/ACCESS.2022.3202640.

[6] E. M. Lizarraga, G. N. Maggio, and A. A. Dowhuszko, "Hybrid beamforming algorithm using reinforcement learning for millimeter wave wireless systems," in *2019 18th Workshop on Information Processing and Control, RPIC 2019*, IEEE, Sep. 2019, pp. 253–258. doi: 10.1109/RPIC.2019.8882140.

[7] A. F. Molisch *et al.*, "Hybrid Beamforming for Massive MIMO: A Survey," *IEEE Communications Magazine*, vol. 55, no. 9, pp. 134–141, 2017, doi: 10.1109/MCOM.2017.1600400.

[8] G. M. Zilli and W. P. Zhu, "Constrained-SVD based Hybrid Beamforming Design for Millimeter-Wave Communications," in *IEEE Vehicular Technology Conference*, IEEE, Nov. 2020, pp. 1–5. doi: 10.1109/VTC2020-Fall49728.2020.9348822.

[9] A. Y. Hassan and A. Saleh, "The Effect of the Eigenvalues of the Zero-Forcing Detector on its Performance in the Space-Division Multiplexing System," *International Journal of Intelligent Engineering and Systems*, vol. 14, no. 1, pp. 340–355, Feb. 2020, doi: 10.22266/IJIES2021.0228.32.

[10] Y. Mao, O. Dizdar, B. Clerckx, R. Schober, P. Popovski, and H. V. Poor, "Rate-Splitting Multiple Access: Fundamentals, Survey, and Future Research Trends," *IEEE Communications Surveys and Tutorials*, vol. 24, no. 4, pp. 2073–2126, 2022, doi: 10.1109/COMST.2022.3191937.

[11] F. Gómez-Cuba and M. Pena-Sande, "Successive Interference Cancellation Implementation for ns-3 MU-MIMO mmWave Module," in *ACM International Conference Proceeding Series*, New York, NY, USA: ACM, Jun. 2024, pp. 45–53. doi: 10.1145/3659111.3659117.

[12] M. A. Albreem, A. H. A. Habbash, A. M. Abu-Hudrouss, and S. S. Ikki, "Overview of Precoding Techniques for Massive MIMO," *IEEE Access*, vol. 9, pp. 60764–60801, 2021, doi: 10.1109/ACCESS.2021.3073325.

[13] N. Fatema, G. Hua, Y. Xiang, D. Peng, and I. Natgunanathan, "Massive MIMO Linear Precoding: A Survey," *IEEE Systems Journal*, vol. 12, no. 4, pp. 3920–3931, Dec. 2018, doi: 10.1109/JSYST.2017.2776401.

[14] N. Iswarya and L. S. Jayashree, "A Survey on Successive Interference Cancellation Schemes in Non-Orthogonal Multiple Access for Future Radio Access," *Wireless Personal Communications*, vol. 120, no. 2, pp. 1057–1078, Sep. 2021, doi: 10.1007/s11277-021-08504-1.

[15] C. Dumas, L. Salaun, I. Hmedoush, C. Adjih, and C. S. Chen, "Design of Coded Slotted ALOHA with Interference Cancellation Errors," *IEEE Transactions on Vehicular Technology*, vol. 70, no. 12, pp. 12742–12757, Dec. 2021, doi: 10.1109/TVT.2021.3120069.

[16] X. Zhao, M. Li, Y. Liu, T. H. Chang, and Q. Shi, "Communication-Efficient Decentralized Linear Precoding for Massive MU-MIMO Systems," *IEEE Transactions on Signal Processing*, vol. 71, pp. 4045–4059, 2023, doi: 10.1109/TSP.2023.3322827.

[17] B. Kaziu, N. Shanin, D. Spano, L. Wang, W. Gerstacker, and R. Schober, "Approximate Partially Decentralized Linear EZF Precoding for Massive MU-MIMO Systems," in *IEEE Vehicular Technology Conference*, IEEE, Oct. 2024, pp. 1–6. doi: 10.1109/VTC2024-Fall63153.2024.10757832.

[18] L. D. Nguyen, H. D. Tuan, T. Q. Duong, and H. V. Poor, "Multi-user regularized zero-forcing beamforming," *IEEE Transactions on Signal Processing*, vol. 67, no. 11, pp. 2839–2853, Jun. 2019, doi: 10.1109/TSP.2019.2905833.

[19] A. Koc and T. Le-Ngoc, "Full-Duplex mmWave Massive MIMO Systems: A Joint Hybrid Precoding/Combining and Self-Interference Cancellation Design," *IEEE Open Journal of the Communications Society*, vol. 2, pp. 754–774, 2021, doi: 10.1109/OJCOMS.2021.3069672.

[20] A. Abrardo, G. Fodor, and M. Moretti, "Distributed Digital and Hybrid Beamforming Schemes With MMSE-SIC Receivers for the MIMO Interference Channel," *IEEE Transactions on Vehicular Technology*, vol. 68, no. 7, pp. 6790–6804, Jul. 2019, doi: 10.1109/TVT.2019.2918066.

[21] G. Taricco, "Fair Power Allocation Policies for Power-Domain Non-Orthogonal Multiple Access Transmission With Complete or Limited Successive Interference Cancellation," *IEEE Access*, vol. 11, pp. 46793–46803, 2023, doi: 10.1109/ACCESS.2023.3274470.

[22] O. El Ayach, R. W. Heath, S. Abu-Surra, S. Rajagopal, and Z. Pi, "The capacity optimality of beam steering in large millimeter wave MIMO systems," in *IEEE Workshop on Signal Processing Advances in Wireless Communications, SPAWC*, IEEE, Jun. 2012, pp. 100–104. doi: 10.1109/SPAWC.2012.6292865.

[23] X. Wu, D. Liu, and F. Yin, "Hybrid Beamforming for Multi-User Massive MIMO Systems," *IEEE Transactions on Communications*, vol. 66, no. 9, pp. 3879–3891, Sep. 2018, doi: 10.1109/TCOMM.2018.2829511.

[24] M. U. A. Siddiqui, F. Qamar, F. Ahmed, Q. N. Nguyen, and R. Hassan, "Interference Management in 5G and beyond Network: Requirements, Challenges and Future Directions," *IEEE Access*, vol. 9, pp. 68932–68965, 2021, doi: 10.1109/ACCESS.2021.3073543.

[25] J. A. Rice, *Mathematical Statistics and Data Analysis*, 3rd ed. Belmont, CA: Thomson Brooks, 2007.

BIOGRAPHIES OF AUTHORS

Heba Shafeik Kashour Department of Electronics and Communications Engineering, Damascus University, Damascus, Syria. Master's degree in Radio Communications, Higher Institute of Applied Sciences and Technology, HIAST-Damascus 2019. Improving the availability of microwave links in mobile telecommunication systems by analyzing performance indicators measures (applied academic study of (space diversity and ATPC) technologies). Optical and MW transport planning engineer, Syriatel Company. She can be contacted at email: hiba.kashour88@damascusuniversity.edu.sy, hiba.sh.kashour@gmail.com.

Abdelrazak Badawieh Bachelor of Science in Electronic Engineering (1971), Department of Electronic Engineering, Faculty of Mechanical and Electrical Engineering, Damascus University. Ph.D. in Electronic Systems (1976), University of Science and Technology, Montpellier, France. He can be contacted at email: gbadawil@gmail.com.

Ali Ahmad Professor specializing in microwaves within the Department of Communications Technology Engineering at the Faculty of Information and Communications Technology Engineering, Tartous University, received his Ph.D. from Russia in 1992. He can be contacted at email: dr-ali-ahmad@tartous-univ.edu.sy.

Mohammad Rizk Assaf Department of Radiophysics, Tomsk State University, Tomsk 634050, Russian Federation, Telecommunications Department, Higher Institute for Applied Science and Technology (HIAST), Damascus, Syria. He can be contacted at email: md.moh1600@gmail.com, mohammad.assaf@hiast.edu.sy.